

AB

OBSERVATION OF RADIATIVE MUON CAPTURE ON THE PROTON

P. Depommier^a, D.S. Armstrong^c, G. Azuelos^{a,d}, W. Bertl^e, M. Blecher^c, C.-Q. Chen^b, B. Doyle^b, T.P. Gorrings^b, P. Gumplinger^b, M.D. Hasinoff^b, G. Jonkmans^a, J.A. Macdonald^d, S.C. McDonald^f, M. Munro^f, J.M. Poutissou^d, R. Poutissou^d, B.C. Robertson^g, E. Saettler^b, D.G. Sample^b, C. Sigler^c, G.N. Taylor^f and D.H. Wright^b.

^aUniversité de Montréal; ^bUniversity of British Columbia, Vancouver; ^cVirginia Polytechnic Institute and State University, Blacksburg; ^dTRIUMF, Vancouver; ^ePaul Scherrer Institut, Villigen; ^fUniversity of Melbourne; ^gQueen's University, Kingston.

ABSTRACT

Radiative muon capture on the proton has been observed for the first time at TRIUMF.

1. INTRODUCTION

I am very pleased to talk today on radiative muon capture, on the invitation by Pauchy Hwang who was a pioneer in the field, with his master Henry Primakoff^{1,2}. Here I would like to share with you some recollections.

When I started working at TRIUMF, in the early seventies, Henry Primakoff was visiting the University of British Columbia, in Vancouver. I paid a visit to him and asked for his opinion about the best experiments to do at TRIUMF. He went to the blackboard and wrote:

- $\mu \rightarrow e\gamma$.
- Muonium-antimuonium conversion.
- Radiative muon capture on the proton.

The first two experiments were undertaken rather soon. In 1973, I proposed a search for the $\mu \rightarrow e\gamma$ at TRIUMF. I remember that Ernest Henley was on the Experiments Evaluation Committee which recommended it. We obtained

a limit of $\sim 10^{-9}$ and later concentrated on the muon-electron conversion in titanium which led to an upper limit of 4.6×10^{-12} . Of course the $\mu \rightarrow e\gamma$ was also searched for at PSI and LAMPF, the best upper limit being 4.9×10^{-11} at LAMPF. The muonium-antimuonium conversion has been (and is still) studied at the meson factories.

The situation has been different for the radiative muon capture on the proton (RMCH). It took about ten more years to see a proposal. The experiment was proposed at TRIUMF by Georges Azuelos about ten years ago. Tony Thomas was on the Experiments Evaluation Committee which accepted it. We had to build a new detector, then to understand all the problems related to the various backgrounds and to the determination of the efficiency. We are now reaching the stage of completion. Why did it take so long?

Here I would like to comment briefly on the difficulties of the experiment. RMCH is the process:

$$\mu^- p \rightarrow \nu_\mu n \gamma$$

It is very rare. Ordinary muon capture on the proton (OMCH) is already $\sim 10^3$ slower than muon decay and RMCH is another $\sim 10^4$ down.

Obviously, it is impractical to detect the neutrino, and it is useless to try to detect the neutron. The latter has a maximum energy of 5 MeV, and due to its interaction in the hydrogen target the information on direction and energy would be completely lost. Moreover, ordinary muon capture, which is $\sim 10^4$ more frequent, produces 5 MeV neutrons. Therefore only the photon is of interest. Its energy spectrum extends from 0 to 100 MeV. But, muon decay has an electron spectrum which extends up to 53 MeV and so does the external Bremsstrahlung spectrum. There is also the radiative muon decay ($B.R. = 1.4 \times 10^{-2}$) which contributes to the photon spectrum below 53 MeV. These sources of background are so large that it is impossible to measure a RMCH photon spectrum below 53 MeV, and even below ~ 58 MeV, due to the finite energy resolution of the detector. One is left with the energy range 58 - 100 MeV. This limitation in energy is a high price to pay. Moreover, in this energy region, the shape of the photon spectrum is not very sensitive to the various form factors. Therefore, only the integrated spectrum can be used. This means that one has to measure the absolute branching ratio of RMCH ($E_\gamma > 58$ MeV). One serious problem is the determination of the detection efficiency (detector acceptance) with a sufficient accuracy.

For such a rare decay there are many dangerous sources of background. We have already discussed the unavoidable background from muon decay (radiative muon decay and external Bremsstrahlung). Cosmic rays give a significant contribution, as well as the ambient radiation which is always present in the vicinity of a particle accelerator. Residual pions in the beam produce a large background which can only be eliminated with a timing cut. Muons can stop in various detector components surrounding the hydrogen (gold and silver). Again, timing and geometrical cuts must be used. The timing cut is another heavy price to pay.



CERN LIBRARIES, GENEVA

swg40

Impurities in the hydrogen cannot be tolerated. Even deuterium must be avoided. The hydrogen has to be pure protium (mass-one hydrogen). If deuterium is present there will be muon-catalysed fusion reactions which produce ${}^3\text{He}$, and the ${}^3\text{He}$ signal adds to the hydrogen signal (muon capture goes approximately like Z^4).

Considering all the factors (branching ratio, reduction due to the various cuts and detector efficiency, we expect one good RMCH event for $\sim 10^{10}$ incident muons.

II. THE PHYSICS

The Standard Model of electroweak interactions describes muon capture at the quark-lepton level. At low energy, the hamiltonian can be reduced to a four-fermion contact interaction with the $V - A$ form:

$$H = \frac{G_F}{\sqrt{2}} [\bar{d}\gamma^\mu(1 - \gamma^5)u][\bar{\nu}_\mu\gamma_\mu(1 - \gamma^5)\mu]$$

But quarks do not exist in the free state, and therefore one can only observe muon capture at the hadron-lepton level. Here, the situation is more complicated, due to the presence of the strong interaction. The latter is believed to be described by Quantum Chromodynamics, but this theory is not very predictive in the non-perturbative regime, as it is the case at low energy. Traditionally, one parametrizes the hadronic matrix elements in terms of form factors, which are functions of the momentum transfer squared. Using standard notations³, we have, for the hadronic matrix elements of the vector and axial-vector matrix elements:

$$\langle n | J_\mu^{(V)} | p \rangle = \bar{u}_n \left[F_V(q^2)\gamma_\mu + F_M(q^2)\frac{1}{2M}\sigma_{\mu\nu}q^\nu + \frac{1}{m_l}F_S(q^2)q_\mu \right] u_p$$

$$\langle n | J_\mu^{(A)} | p \rangle = \bar{u}_n \left[F_A(q^2)\gamma_\mu\gamma^5 + F_T(q^2)\frac{1}{2M}\sigma_{\mu\nu}\gamma^5q^\nu + \frac{1}{m_l}F_P(q^2)\gamma^5q_\mu \right] u_p$$

where M is the nucleon mass and m_l the lepton mass. u_p and \bar{u}_n are Dirac spinors.

The Standard Model, symmetry arguments and experimental results allow us to reduce the number of unknown form factors:

- Assuming time-reversal invariance in the first generation of quarks and leptons, all form factors can be chosen as real functions of q^2 .
- The Standard Model does not predict the existence of second-class currents, therefore we take $F_S(q^2) \equiv 0$ and $F_T(q^2) \equiv 0$.
- Using the conservation of the vector current (CVC), which is an ingredient of the Standard Model, one relates the form factors $F_V(q^2)$ and $F_M(q^2)$ to the electromagnetic form factors, which are well measured by electron scattering.

- The β decay of the neutron provides us with a value of $F_A(q^2 = 0)$. The q^2 dependence of $F_A(q^2)$ is known from experiment^{4,7}. For our purpose it is a small effect.

Therefore we are left with the pseudoscalar form factor $F_P(q^2)$, which is the subject of our experimental study.

The pseudoscalar form factor has been studied theoretically in the context of the Partial Conservation of Axial Current (PCAC hypothesis). The pion plays a special role in this theoretical treatment.

Using additional assumptions on the q^2 dependence of the form factors, one gets the Goldberger-Treiman relation for g_P :

$$g_P(q^2) = \frac{2m_\mu g_{\pi NN} F_\pi}{m_\pi^2 + q^2} = \frac{2M m_\mu}{m_\pi^2 + q^2} g_A(0)$$

According to a recent experimental result⁷ the momentum-transfer dependence of g_P is well explained by the pion-pole dominance.

Numerically:

$$g_P(0.88m_\mu^2) = 7.1g_A(0)$$

where g_A and g_P are defined as:

$$g_A(q^2) = F_A(q^2) \quad g_P(q^2) = \frac{F_P(q^2)}{m_\mu}$$

The choice of $q^2 = 0.88m_\mu^2$ corresponds to the fact that in OMCH the momentum transfer has this particular value.

A new calculation of g_P ⁸ has appeared recently. It is based on the chiral Ward identities of QCD and heavy-baryon chiral perturbation theory:

$$g_P = \frac{2m_\mu g_{\pi NN} F_\pi}{m_\pi^2 + 0.88m_\mu^2} - \frac{1}{3}g_A m_\mu M \tau_A^2$$

where m_μ , m_π and M are the masses of the muon, pion and nucleon, respectively; τ_A^2 is the mean square axial radius of the nucleon. This result was obtained a long time ago by Wolfenstein^{9,10}, using a once-subtracted dispersion relation. But it now rests on a firmer theoretical ground.

Using as input values the well-known masses m_π , m_μ and M , and:

$$F_\pi = (92.5 \pm 0.2) \text{ MeV}$$

$$g_A = 1.2573 \pm 0.0028$$

$$g_{\pi NN} = 13.31 \pm 0.34$$

$$r_A = (0.65 \pm 0.03) \text{ fm} = (3.30 \pm 0.15) \text{ GeV}^{-1}$$

one obtains⁸:

$$g_P = (8.89 \pm 0.23) - (0.45 \pm 0.04) = 8.44 \pm 0.23$$

Considering the accuracy of this theoretical prediction, it is urgent to measure g_P to an accuracy of 2%.

There is another reason to measure g_P on the proton. Radiative muon capture can also be used as a probe for nuclear structure. In fact it is now possible to make accurate and reliable measurements of RMC on nuclei¹¹ since the capture rate is large, especially in medium-mass and heavy nuclei. The question of a possible renormalization of g_P in the nuclear medium has not been fully clarified¹². New developments have appeared recently¹³.

The importance of muon capture for the determination of g_P has been stressed many times. It has also been noticed that RMC is more sensitive than OMC to g_P . The reason is that in RMC the photon spectrum can be measured in a region where the momentum transfer $q^2 \sim -m_\mu^2$, therefore one gets closer to the pion pole.

The theory of RMC has been developed by several authors^{14,15,16}. The influence of the Δ resonance has been included^{17,18}. It gives a 10% enhancement near the energy end-point (only a few per-cent on the branching ratio).

III. THE TRIUMF EXPERIMENT

A. Choosing the detector

To detect high-energy photons the obvious choice would be an electromagnetic calorimeter. One would use a homogenous calorimeter made of inorganic scintillator, for instance sodium iodide. They have a good detection efficiency and a fairly good energy resolution. Several experiments have used sodium iodide crystals to study RMC on complex nuclei (a more favorable situation for the competition capture vs decay). But for RMCH sodium iodide crystals cannot be used. The reason is that they are also sensitive to neutrons. There are always many neutrons in the vicinity of a particle accelerator, and the OMCH process produces neutrons in abundance in comparison to RMCH.

On the other hand, pair spectrometers have been used to detect high-energy photons. They have very good energy resolution but normally very small solid angles. They are insensitive to neutrons in the energy region of interest.

We have opted for a pair spectrometer with a large solid angle and a resolution which is comparable to that of a sodium iodide crystal.

Figure 1 shows the detector. It surrounds the protium target and covers a solid angle $\Omega \sim 0.75 \times 4\pi$. Several scintillation counters (A, A' and B) act as vetos to reject charged particles. Photons are converted into electron-positron pairs in a lead converter (1 mm thick). The pairs will trigger the scintillation counters C and D and will be tracked in a drift chamber.

The drift chamber (see Figure 2) consists of four layers of sensitive cells. Each cell has six sensitive wires. The ionization electrons drift towards the

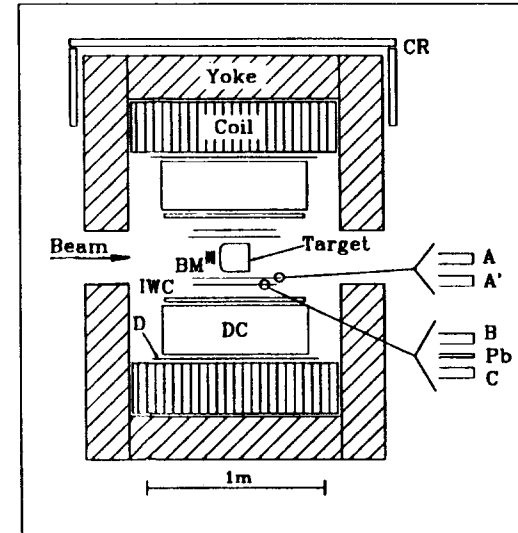


Figure 1: The TRIUMF pair spectrometer used for the study of radiative muon capture on the proton.

sensitive wires and the drift time is measured. This gives a number of coordinate pairs (radius r , azimuth ϕ). The z coordinate (along the axis of the detector) is measured at two locations. Firstly, there is a cylindrical multi-wire proportional chamber (IWC). Secondly, the third layer of the large drift chamber is used in the stereo mode. This give two values of z .

A detailed description of the detector is given in references^{19,20}.

B. The protium target

In order to get a sufficient density, to stop enough muons, we decided to use a liquid hydrogen target. The price to pay is the complexity of the muon chemistry in liquid hydrogen.

As explained above we must use a pure protium target, which must also be exempt of any heavier impurities. The protium was obtained from the electrolysis of pure light water. The deuterium contamination was measured by mass spectrometry and amounted to less than 2 ppm. Even with this deuterium concentration a correction is necessary. To determine it, runs have been taken with protium contaminated with a known quantity of deuterium. The protium is recirculated and purified at the beginning of each running period.

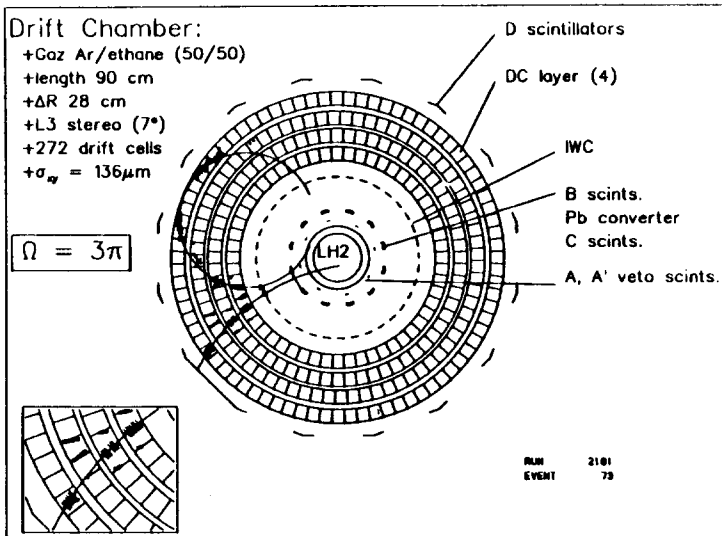


Figure 2: An electron-positron pair in the RMC detector.

Liquid hydrogen must be kept in a container. Even with a careful design of the target to minimize the number of muon stops in the walls, RMC in the walls constitutes a major source of background. By choosing for the target walls a heavy material (like gold) it is possible to eliminate this background with a time cut. The muon lifetime is very short in heavy elements (72.6 ns. in gold, 88.7 ns. in silver), whilst it is much longer in hydrogen (2194.9 ns.). This time cut is another high price to pay.

C. The trigger

The following conditions are required for an event which will be written to tape:

- The initial particle is not charged. The scintillation counters A, A' and B should be silent.
- There should be a signal in one of the scintillation counters C and at least one in the scintillation counters D. Note that we do not require two D signals since we want to accept events where only one particle of the pair reaches the D counters, the other one wrapping around (see figure 2).

D. The muon beam

In order to minimize the number of muon stops in other elements than hydrogen the beam must be well focused. The stopping distribution must be known precisely since it is used in the Monte Carlo calculation.

It is absolutely essential for the experiment to purify the muon beam from the pion and electron contaminants. This is done with an electromagnetic separator. Since the muons, pions and electrons arrive at different times at the separator, the latter acts as a gate which allows the muons to pass, but not the pions nor the electrons. The pion contamination is brought down to 10^{-3} but this is not sufficient and the background from pion capture is still the dominant contribution in the raw data (see Figure 3).

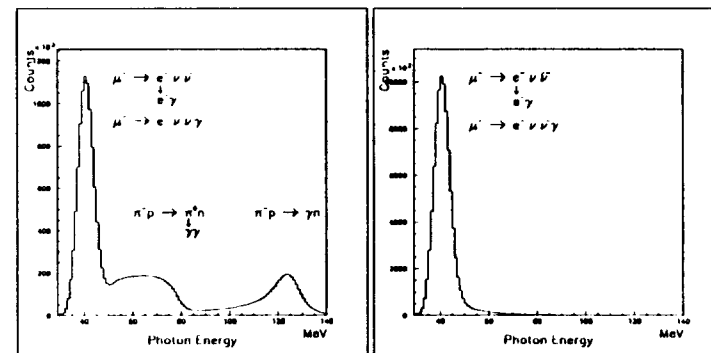


Figure 3: The situation before and after the "prompt" cut.

E. The cosmic-ray shield

To reduce the cosmic-ray background one uses scintillation counters and proportional chambers in anti-coincidence.

IV. REDUCTION OF THE DATA

A. The selection criteria

To eliminate (or reduce) certain sources of background, successive criteria are applied.

In a first step, one selects good electron and positron tracks and identifies a corresponding good photon.

- The tracking cuts: they are used to reject particle tracks (electrons, positrons) which are badly reconstructed (mainly due to multiple scattering in the drift chamber) and which would damage the energy resolution. These cuts are efficient in reducing the high-energy tail of the photon spectra from Bremsstrahlung and radiative muon decay, and also the cosmic-ray background.
- The photon cuts: they are used to make sure that the two tracks (electron and positron) come from a photon. Accidental events due to pile-up are thus eliminated.
- The geometrical cuts: the aim is to obtain information on the origin of the photon, to eliminate photons which come from the lead collimator and other materials outside the target region. Cuts imposed on several geometrical parameters are efficient in reducing the background coming from radiative muon capture in the walls of the hydrogen target and in the lead collimator located before the target. The cosmic-ray background is also reduced.
- The random cuts: they are used to eliminate accidental coincidences which could simulate good photons.
- The cosmic cuts: the aim is to reduce cosmic-ray events which simulate good photons. In fact, the background also include events which are induced by the ambient radiation in the experimental hall. We have been able to correlate the magnitude of this background with the intensity in the meson-production line.

At that point, a good event consisting of only one photon is defined.

In the second step, one selects the events which are due to the RMCH process.

- The pion cut: the aim is to reject photons due to radiative pion capture ($\pi^-p \rightarrow \gamma n$) and to pion charge exchange ($\pi^-p \rightarrow \pi^0 n$) followed by neutral pion decay ($\pi^0 \rightarrow \gamma\gamma$) in flight. Since these events are prompt (they coincide in time with a pion stop) a timing cut is applied. Also the amount of energy deposited in the beam counters is used to identify pions versus muons. The effect of this cut is to eliminate all events due to residual pions.
- The blank cut: the aim is to eliminate RMC photons produced in the materials surrounding the hydrogen (mainly silver and gold). The separation is made on the basis of the very different lifetimes of the muon in these elements: gold (76.2 ns.), silver (88.7 ns.) and hydrogen (2194.9 ns.). A lifetime fit to the events gives the composition of the event sample. A timing cut reduces the contribution of the heavy elements to a small amount.

- The energy cut: finally, the branching ratio is evaluated above a cut-off energy (~ 57 MeV). The behavior of the branching ratio as a function of the cut-off energy is investigated.

V. THE DETECTION EFFICIENCY

To determine the detection efficiency, i.e. the probability that a photon of a certain energy is accepted by the detector and the selection criteria, one makes use of a well-known and abundant process: negative pion capture on the proton. Essentially there are two processes:

$$\pi^- p \rightarrow \gamma n \quad 38.6\% \quad \pi^- p \rightarrow \pi^0 n \quad 60.7\%$$

The first one gives a photon of 129 MeV and the second a photon spectrum which has a constant value in the range 55-82 MeV. The experimentally observed spectrum agrees reasonably well with the Monte Carlo prediction.

To do a calibration run, the beam line is tuned to accept low-energy negative pions. It takes only a short time to obtain an energy spectrum (see Fig. 4). The pion-induced events are analysed with the same cuts as the muon-induced events. Knowing the number of pion stops, it is straightforward to evaluate the detection efficiency (detector acceptance) as a function of photon energy.

VI. THE RMCH PHOTON SPECTRUM AND BRANCHING RATIO

The experimentally observed photon spectrum (events which survive all cuts) is shown on figure 5

For the determination of the branching ratio the ingredients are: the number of RMCH events above a certain energy (obtained from the analysis of the data); the corresponding detection efficiency (obtained from the pion runs); the number of muon stops (obtained from the scalers after appropriate corrections). The result is the branching ratio for $E_\gamma > E_0$. It has the value (still preliminary since it is based on a fraction of the data):

$$\text{B.R. (RMCH; } E_\gamma > 60 \text{ MeV)} = \frac{\text{Events}}{\text{Acceptance} \times \text{Stops}} = (1.6 \pm 0.3) \times 10^{-8}$$

where:

$$\text{Events} = 250 \pm 21 \quad \text{Acc} = 0.5\% \quad \text{Stops} = 3.21 \times 10^{12}$$

VII. FROM THE BRANCHING RATIO TO g_p

A. The physics

There are several considerations to take into account. First, there is the capture process on the proton. It has been calculated several times and

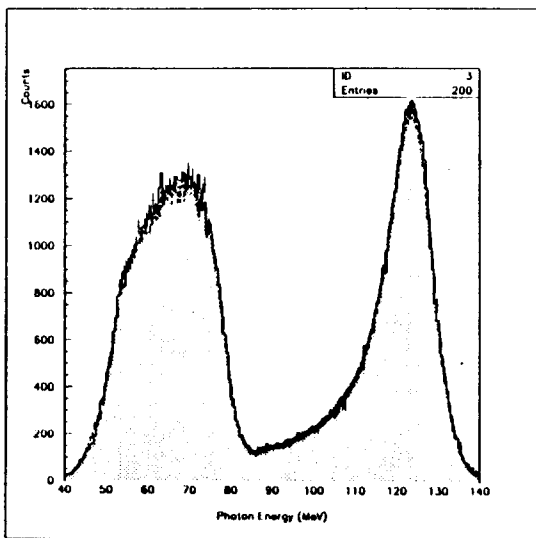


Figure 4: Photon energy spectrum following pion capture on the proton: experiment and Monte Carlo prediction.

most of the results are in good agreement. In our study we use the computer program written at TRIUMF by H. Fearing.

B. The input parameters

The following values of the various form factors have been used:

$$g_V = 1.0 \quad g_M = 3.706 \quad g_A = 1.2573$$

C. The muonic chemistry

Since we use a liquid hydrogen target we must consider the capture probabilities from the various atomic and molecular states. The value of g_P is somewhat sensitive to the various input parameters, like the ortho-para transition rate, for which we have an experimental value²¹:

$$\lambda_{op}^{exp} = (4.1 \pm 1.4) \times 10^4 s^{-1}$$

and a theoretical value²²:

$$\lambda_{op}^{th} = (7.1 \pm 1.2) \times 10^4 s^{-1}$$

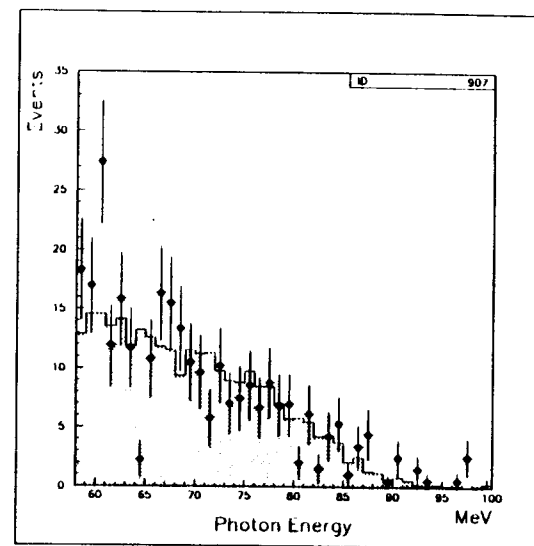


Figure 5: Photon energy spectrum of radiative muon capture on the proton.

Also we need the parameters which describe the muon density at the proton in the (ortho and para) molecular states²²:

$$f_o^{mol} = 1.01$$

$$f_p^{mol} = 1.15$$

VIII. CONCLUSION

We have observed radiative muon capture on the proton for the first time. The analysis of the data is continuing and we expect a final result with an accuracy $\sim 10\%$. Building on our experience we think that it will be possible to perform a better experiment with an accuracy $\sim 3\%$, comparable to the uncertainty of the theoretical prediction.

REFERENCES

1. W.-Y. P. Hwang and H. Primakoff. *Phys. Rev.*, **C18** (1978) 414.
2. W.-Y.P. Hwang and H. Primakoff. *Phys. Rev.*, **C18** (1978) 445.
3. N.C. Mukhopadhyay. Study of fundamental interactions with nuclear muon capture. In P. Deponnmer, editor, *Proceedings of the International Conference*

- on *Weak and Electromagnetic Interactions in Nuclei (Montreal, May 1989)*, page 51. Editions Frontières, 1989.
4. A. Delguerra et al. *Nucl. Phys.*, **B107** (1976) 65.
 5. A.S. Esauslov et al. Longitudinal and transverse contributions to the threshold cross-section slope of single-pion electroproduction by a proton. *Nucl. Phys.*, **B136** (1978) 511.
 6. L.A. Ahrens et al. A study of the axial-vector form factor and second-class currents in antineutrino quasielastic scattering. *Phys. Lett.*, **B202** (1988) 284.
 7. Sionho Choi et al. Axial and pseudoscalar nucleon form factors from low energy pion electroproduction. *Phys. Rev. Lett.*, **71** (1993) 3927.
 8. V. Bernard, N. Kaiser, and Ulf-G. Meissner. "QCD accurately predicts the induced pseudoscalar coupling constant". Preprint CRN-94/13, Centre de Recherches Nucléaires et Université Louis Pasteur, Strasbourg, B.P. 20, F-67037 Strasbourg CEDEX 2, France.
 9. L. Wolfenstein. In S. Devons, editor, *High-Energy Physics and Nuclear Structure*, page 661. Plenum Press, New York, (1970).
 10. H. Pagels. *Phys. Rev.*, **179** (1969) 1337.
 11. D.S. Armstrong et al. *Phys. Rev.*, **C43** (1991) 1425.
 12. H.W. Fearing and M.S. Welsh. Radiative muon capture in medium heavy nuclei in a relativistic mean field theory model. *Phys. Rev.*, **C46** (1992) 2077.
 13. J. Delorme and M. Ericson. s-wave pion-nucleus interaction and weak coupling constants. *Phys. Rev.*, **49** (1994) R1763.
 14. K. Huang, C.N. Yang, and T.D. Lee. *Phys. Rev.*, **108** (1957) 1348.
 15. G.I. Opat. Radiative muon capture on hydrogen. *Phys. Rev.*, **B134** (1964) 428.
 16. Harold W. Fearing. Relativistic calculation of radiative muon capture in hydrogen and ^3He . *Phys. Rev.*, **C21** (1980) 1951.
 17. D.S. Beder and H.W. Fearing. Contribution of the Δ (1232) to $\mu^-p \rightarrow n\nu\gamma$. *Phys. Rev.*, **D35** (1987) 2130.
 18. D.S. Beder and H.W. Fearing. Radiative muon capture in hydrogen and nucleon excitation. *Phys. Rev.*, **D39** (1989) 3493.
 19. R.S. Henderson et al. *IEEE Transactions on Nuclear Science*, **37** (3) (1990) 1116.
 20. D.H. Wright et al. *Nucl. Inst. and Meth.*, **A320** (1992) 249.
 21. G. Bardin et al. *Phys. Lett.*, **104B** (1981) 320.
 22. D.D. Bakalov et al. *Nucl. Phys.*, **A384** (1982) 302.

